A Fractal Model for Effective Excess Charge Density in Variably Saturated Fractured Rocks

Luis Guarracino, Damien Jougnot

A fractal model for effective excess charge density in variably saturated fractured rocks

Luis Guarracino[1] **and Damien Jougnot**[2]

[1]Consejo Nacional de Investigaciones Científicas y Técnicas, Facultad de Ciencias Astronómicas y Geofísicas, Universidad Nacional de La Plata, Paseo del Bosque s/n, La Plata (1900), Argentina
[2]Sorbonne Université, CNRS, EPHE, UMR 7619 Metis, F-75005, Paris, France

Key Points:

- A conceptual model is proposed to describe effective excess charge density in fractured media
- The model is based on physical principles and a fractal description of fracture networks
- Model expressions in terms of hydraulic variables are identical to those obtained for classic porous media

Corresponding author: Luis Guarracino, luisg@fcaglp.unlp.edu.ar

Abstract

Estimating hydraulic properties and monitoring water flow in fractured rocks using self-potential observations essentially relies on our ability to model streaming potential. One of the most promising approaches for modelling electrokinetic couplings is based on the macroscopic quantification of the excess charge which is effectively transported by pore water flow. In this study, we derive a fractal model to predict the effective excess charge density for fully and partially water saturated fractured media. Fractures are conceptualized as parallel plates with a fractal pattern described by the Sierpinski carpet. From the calculation of the excess charge in a single fracture and a flux averaging upscaling procedure, we obtain closed-form expressions for the effective excess charge density. This new analytical model explicitly depends on the fracture water ionic concentration, interface properties, water saturation, porosity and permeability. Model predictions under saturated conditions are compared to published data measured in laboratory during hydraulic fracturing. The model development also shows the independence of the excess charge from the pore shapes: when expressed in terms of hydrological parameters, one can find an expression identical to recently published models for sedimentary porous media using capillary tubes. These results extend the validity of the existing models to fractured rocks and highlight the importance of hydraulic parameters for an accurate modelling of electrokinetic couplings.

Plain Language Summary

Groundwater flow in fractured rocks can be indirectly monitored by measuring the electrical potential distribution in the medium or at its surface. The water flow within each fracture drags electrical charges that produce variations in the electrical field. Then, to quantitatively study the water flow from self-potential measurements, we need a theoretical model that links the hydraulic and electrical properties of fractured rocks. In this study, we present a theoretical development of a key parameter called the effective excess charge density. It quantifies the electrical potential generated by water flow. To calculate this parameter, we assume a fracture network with a fractal distribution, that is, a pattern of fractures that repeats itself at different spatial scales. From the description of the drag of electrical charges in a single fracture we estimate a value of the effective excess charge density which is representative of the whole fractured rock. The model results in rather simple mathematical expressions depending on the chemical composition of water, solid-water interface properties, porosity, degree of saturation, and permeability of the rock. To validate the proposed model, our theoretical predictions are compared with experimental laboratory data. This new model opens-up possibilities of using self-potential data for monitoring complex processes like hydraulic fracturing.

1 Introduction

Fractured rocks are a particular type of porous media usually composed of an impermeable or low-permeable matrix with a network of interconnected fractures. Hydraulic characterization of this type of rocks is of interest for a wide range of problems, including groundwater contamination, hydraulic fracturing, CO_2 sequestration and nuclear waste storage (e.g., Medici et al., 2019; Osiptsov, 2017; Ren et al., 2017; Bodvarsson et al., 1999). Few geophysical techniques can provide non-invasive means to study the water flow in fractured media but they are mostly still under development. These techniques include the analysis of seismic attenuation produced by wave-induced fluid flow and associated seismoelectrical signals (e.g., Rubino et al., 2013; Jougnot et al., 2013; Rosas-Carbajal et al., 2020), ground penetrating radar (e.g., Shakas et al., 2018), electrical resistivity tomography (e.g., Roubinet & Irving, 2014; Demirel et al., 2018), and the self-potential method (e.g., Roubinet et al., 2016; Jougnot et al., 2020).

The streaming potential is the contribution of the self-potential signal that is generated by fluid flow. One of the first experimental evidences of the electrokinetic potential generated in fractured rocks is associated with earthquakes. Anomalous variations of self potential have been observed prior to the occurrence of earthquakes (Sobolev, 1975; Corwin & Morrison, 1977). Mizutani et al. (1976) proposed an electrokinetic mechanism for these variations induced by diffusion of groundwater into the dilatant focal region. Then, Yoshida et al. (1998) provided strong evidences of an electrokinetic origin by demonstrating that self-potential markedly changes prior to rupture in saturated basalt specimens, whereas no signal is detected in dry basalts. More recently, researches have shown the interest of in situ streaming potential to detect flow in fractured groundwater reservoirs (e.g., Fagerlund & Heinson, 2003; Maineult et al., 2013), identify the orientation of hydraulically active fracture (Wishart et al., 2006, 2008; Roubinet et al., 2016), or to localize water leakage resulting from hydraulic fracturing (Revil et al., 2015).

The aim of this study is to develop a fractal-based model to describe the electrokinetic coupling phenomena in fractured media using the effective excess charge approach (e.g., Revil & Jardani, 2013; Jougnot et al., 2020). This is a key parameter to calculate streaming potential, that is, the contribution to the self-potential signal due to the drag of electrical charge by water flow inside fractures. The fracture surfaces are usually electrically charged and form electrical double layer (EDL) at the solid-water interface (e.g., Leroy & Revil, 2004). This layer contains an excess of charge in water that compensates the charge deficiency of the fracture surface. The EDL can be decomposed into the Stern and diffuse layers. The Stern layer is very thin and contains only counterions that cover the mineral surface. The diffuse layer contains an unbalanced amount of counterions with a net excess charge. The streaming current is generated by water flow inside fractures that drags a fraction of this excess charge. Following the approach originally proposed by Sill (1983) and modified by Kormiltsev et al. (1998) and Revil et al. (2007), the electrical potential φ (V) distribution and the Darcy velocity $\mathbf{v}_D$ (m s^{-1}) are related through the following macroscopic equation:

$$\nabla \cdot (\sigma \nabla \varphi) = \nabla \cdot \left(\hat{Q}_v \mathbf{v}_D \right) \tag{1}$$

where, $\hat{Q}_v$ is the effective excess charge density (C m^{-3}) and σ is the electrical conductivity (S m^{-1}). The streaming potential SP (V) is then the electrical potential difference between the electrical potential at a given point φ_i and the one at the reference φ_{ref}: $SP = \varphi_i - \varphi_{ref}$.

An alternative approach to quantify the streaming potential is based on the coupling coefficient C_c, a petrophysical property that relates fluid pressure (P) and electrical potential gradients: $C_c = \Delta\varphi/\Delta P$ (Helmholtz, 1879; Smoluchowski, 1903). The coupling coefficient C_c (V Pa^{-1}) is related to $\hat{Q}_v$ through the following relation (e.g., Revil & Leroy, 2004; Jougnot et al., 2012, 2020):

$$C_c = -\frac{\hat{Q}_v k}{\sigma \eta} \tag{2}$$

where k (m^2) is the permeability of the medium and η (Pa s) the fluid dynamic viscosity.

The main assumption of the proposed electrokinetic model is that the fracture network has a fractal pattern. Fractal objects display self-similarity in their geometry, this means that the pattern observed in a small portion of the object is a replica of the whole at a larger scale. In nature, fractures exist over a wide range of scales, from microns to thousands of kilometers, and fractal patterns have been reported by many researchers (e.g., Bonnet et al., 2001; Okubo & Aki, 1987). In this study, the fracture pattern is described by a Sierpinski carpet, which is a plane fractal that contains a self-similar geometric pattern of holes. This specific fractal pattern has been detected in fractured coal

samples using micro X-ray tomography (Zhou et al., 2018; Wu et al., 2019), and successfully used to derive constitutive models for variably saturated flow in fractured rocks (e.g., Guarracino, 2006; Monachesi & Guarracino, 2011; Wang et al., 2017).

The equivalent medium theory is used to estimate the effective excess charge for fractured media, following the flux-averaging approach proposed by (Jougnot et al., 2012). First, the effective excess charge in a single fracture is calculated from the spatial distribution of both the excess charge in the diffuse layer and the water velocity profile. Then the effective excess charge density at the macroscopic scale $\hat{Q}_v$ is estimated using an upscaling procedure based on the integration of the excess charge of all network fractures. By combining this result and the hydraulic properties derived in Guarracino (2006) and Monachesi and Guarracino (2011) for the same fracture network, we obtain a closed-form expression for $\hat{Q}_v$ in terms of permeability, porosity, saturation and electrokinetic parameters. This modeling strategy has been successfully used for estimating $\hat{Q}_v$ in classical porous media described by capillary tubes (e.g., Guarracino & Jougnot, 2018; Soldi et al., 2018, 2020; Jougnot et al., 2019; Rembert et al., 2020).

Note that this new effective excess charge density model for fractured media is based geometric parameters (i.e., fracture aperture, length, recursion-based construction) that are fundamentally different from capillary tubes (i.e., capillary radius, pore throat). However, the analytical expressions of both models become identical when expressed in terms of macroscopic hydraulic parameters (i.e., permeability, porosity and saturation). This result highlights the intrinsic importance of hydraulic characterization in the analysis of self-potential in any type of porous media. Interpretation of self-potential data in fractured media is often qualitative and based on a visual correlation between signal anomalies and observed fracture orientations. This is the first analytical model that consistently describes both electrokinetic and hydraulic properties in fractured rocks and represents a step forward in the quantitative interpretation of self-potential signals.

2 Conceptual model

2.1 Description of the fractured media

To derive the effective excess charge density model we consider the geometrical description of fractured media proposed by Guarracino (2006). The representative elementary volume (REV) is assumed to be a cube of volume a^3 (see Fig. 1b). The voids of the REV are parallel and vertical fractures of length a and aperture b with a horizontal self-similar pattern described by a Sierpinski carpet (Fig. 1). The upper and lower cut-offs for the fractal behavior are defined by the largest (b_{max}) and smallest (b_{min}) apertures observed in the REV.

A Sierpinski carpet can be geometrically constructed by using recursive algorithms that cut out of the carpet successively smaller pieces in each recursion level (Tyler & Wheatcraft, 1990; Guarracino, 2006). In this study we remove rectangular pieces of length a and aperture b from the carpet in order to obtain fractures with a self-similar pattern. Fig. 2 shows the first 3 levels of recursion for a network of parallel fractures assuming $a = 3$ cm and $b_{max} = 1$ cm.

The geometric pattern of Sierpinski carpet is characterized by the fractal dimension D that can vary between 1 and 2. Assuming that the fracture network is formed by parallel fractures, the fractal dimension can be expressed in terms of the largest fracture aperture b_{max} (Guarracino, 2006):

$$D = \frac{\log\left(\frac{a^2}{b_{max}^2} - \frac{a}{b_{max}}\right)}{\log\left(\frac{a}{b_{max}}\right)}. \tag{3}$$

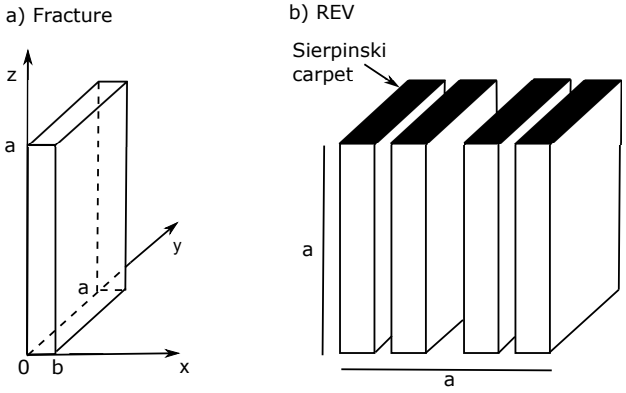

Figure 1. (a) Fracture of aperture b and length a; (b) Representative elementary volume (REV) of the fractured medium.

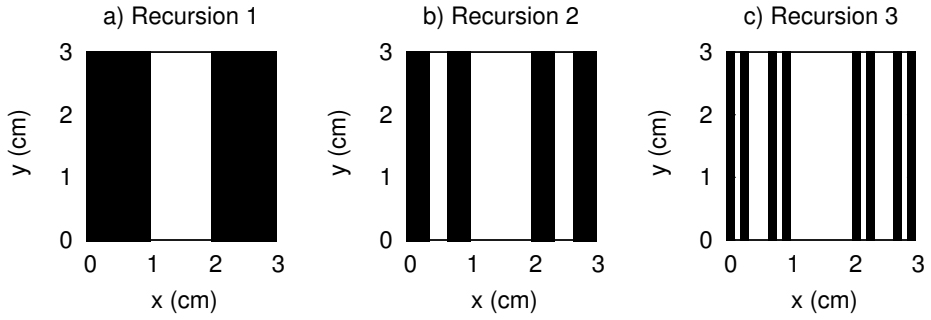

Figure 2. Fracture network generated by 3 recursion levels of a Sierpinski carpet of $D = 1.63$.

Note that the lower limiting value $D = 1$ corresponds to a fracture network whose maximum aperture fills half of the REV ($b_{max} = a/2$) and the upper limiting value $D = 2$ corresponds to an unfractured REV ($b_{max} = 0$). Then, fractal dimension can be used as an indicator of the fracturation degree of the rock matrix.

The fractures of Sierpinski carpet whose apertures are within the infinitesimal range b and $b + db$ cover the following area:

$$dA = (2 - D)a^D b^{1-D} db. \tag{4}$$

The velocity distribution inside a single fracture of aperture b and length a under laminar flow conditions can be described by:

$$v(b, x) = \frac{\rho_w g}{8\eta} \left[b^2 - (b - 2x)^2\right] \frac{\Delta h}{a}, \tag{5}$$

where x (m) is the distance from the fracture wall ($x = 0$) to the center of the fracture ($x = b/2$), ρ_w the water density (kg/m^3), g the gravitational acceleration (m/s^2), η the dynamic viscosity (Pa s), and Δh the pressure or tension head drop across the REV (m). The average velocity $\overline{v}$ (m/s) in the fracture has the following expression:

$$\overline{v}(b) = \frac{\rho_w g}{12\eta} b^2 \frac{\Delta h}{a}. \tag{6}$$

The macroscopic hydraulic properties of the fractured media can be described in terms of the geometrical parameters of a fracture network. In Guarracino (2006) and Monachesi and Guarracino (2011) the following expressions for porosity ϕ, permeability k, saturation S and relative permeability k_r are obtained:

$$\phi = \frac{1}{a^{2-D}} \left(b_{max}^{2-D} - b_{min}^{2-D}\right) \tag{7}$$

$$k = \frac{2 - D}{12a^{2-D}(4 - D)} \left(b_{max}^{4-D} - b_{min}^{4-D}\right) \tag{8}$$

$$S(h) = \frac{h^{D-2} - h_{max}^{D-2}}{h_{min}^{D-2} - h_{max}^{D-2}}, \;\; h_{min} \leq h \leq h_{max} \tag{9}$$

$$k_r(S) = \frac{\left[(b_{max}^{2-D} - b_{min}^{2-D})S + b_{min}^{2-D}\right]^{\frac{4-D}{2-D}} - b_{min}^{D-4}}{b_{max}^{4-D} - b_{min}^{4-D}} \tag{10}$$

where h is the tension head (positive), $h_{min} = 2\sigma \cos(\beta)/\rho g_w b_{max}$, $h_{max} = 2\sigma \cos(\beta)/\rho_w g b_{min}$, σ is the surface tension of water, and β the contact angle.

2.2 Electrokinetic properties of a single fracture

The first step to derive the macroscopic effective excess charge density is to estimate the effective excess charge of a single fracture. Let us consider a fracture of aperture b and length a (see Fig. 1a) saturated by a binary symmetric 1:1 electrolyte (e.g., NaCl) in a laminar flow regime.

The excess charge distribution $\bar{Q}_v$ in the diffuse layer at a distance x of wall fracture can be expressed as (Guarracino & Jougnot, 2018):

$$\bar{Q}_v(x) = N_A e_0 C^0 \left[e^{-\frac{e_0 \psi(x)}{k_B T}} - e^{\frac{e_0 \psi(x)}{k_B T}}\right], \tag{11}$$

where N_A is the Avogadro's number (mol^{-1}), e_0 the elementary charge (C), C^0 the ionic concentration far from the mineral surface (mol/m^3), ψ the local electrical potential in

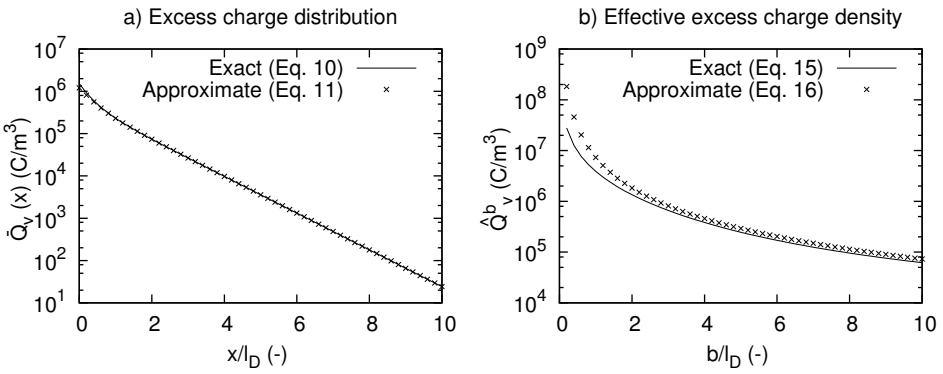

Figure 3. (a) Exact and approximate expressions of the excess charge distribution $\bar{Q}_v(x)$; (b) exact and approximate expressions of the effective excess charge $\hat{Q}^b_v$ for a single fracture of aperture b. The assumed values of ionic concentration, absolute temperature and ζ-potential are $C^0 = 1.0$ mol/m^3, $T = 293.15$ K and $\zeta = -0.07$ V. The distance x and aperture b are scaled by the Debye length l_D.

the fracture water (V), k_B the Boltzman constant (J/K), and T is the absolute temperature (K).

In this study, the exponential terms of (11) are approximated by a four-term Taylor series. Under this approximation, the excess charge distribution can be expressed as:

$$\bar{Q}_v(x) = -2N_A e_0 C^0 \left[\frac{e_0}{k_B T}\psi(x) + \frac{1}{6}\left(\frac{e_0}{k_B T}\psi(x) \right)^3 \right]. \tag{12}$$

Figure 3a shows the excellent agreement between exact and approximate excess charge distributions described by Eq. (11) and (12), respectively.

For the thin double layer assumption the local electrical potential can be expressed (Hunter, 1981):

$$\psi(x) = \zeta e^{-\frac{y}{l_D}}, \tag{13}$$

$$l_D = \sqrt{\frac{\epsilon k_B T}{2N_A C^0 e_0^2}}, \tag{14}$$

where ζ (V) is the ζ-potential on the shear plane, l_D the Debye length (m) which represents a characteristic thickness of the diffuse layer, and ϵ the water dielectric permittivity (F/m).

Based on the ideas presented in Guarracino and Jougnot (2018), the effective excess charge density $\hat{Q}^b_v$ carried by the water flow in a single fracture of aperture b is defined by:

$$\hat{Q}^b_v = \frac{2}{\overline{v}(b)ab}\int_0^{b/2} \overline{Q}_v(x) v(b,x) a \, dx. \tag{15}$$

Then, by substituting (5), (6) and (12) in (15) we obtain:

$$\begin{aligned} \hat{Q}^b_v = \; & -\frac{24 N_A e_0 C^0}{(b/l_D)^2}\left(\frac{e_0\zeta}{k_B T}\right)\left[1 - \frac{2l_D}{b} + e^{-\frac{b}{2l_D}}\left(\frac{2l_D}{b} + \frac{b}{2l_D}\right)\right] \\ & -\frac{12 N_A e_0 C^0}{(b/l_D)^2}\left(\frac{e_0\zeta}{3k_B T}\right)^3\left[1 - \frac{2l_D}{3b} + e^{-\frac{3b}{2l_D}}\left(\frac{2l_D}{3b} - \frac{3b}{4l_D}\right)\right]. \end{aligned} \tag{16}$$

Under the thin double layer assumption, the thickness of the electrical diffuse layer is assumed small compared to fracture aperture ($l_D << b$) and Eq. (16) can be approximated by:

$$\hat{Q}_v^b = \frac{12 N_A e_0 C^0}{(b/l_D)^2} \left[-2\frac{e_0\zeta}{k_B T} - \left(\frac{e_0\zeta}{3k_B T} \right)^3 \right]. \tag{17}$$

Figure 3b shows the very good agreement for $b/l_D > 3$ between exact and approximate excess charge described by Eq. (16) and (17), respectively. In capillary tube models the thin double layer assumption is valid so long as the capillary radius is greater than 200 l_D (Jackson & Leinov, 2012). Assuming that the fracture aperture is 2 times the capillary radius, the validity of the thin double layer assumption for fracture models can be state for apertures $b > 400 l_D$. Moreover, if we consider that in monovalent electrolyte concentrations between 1 mol/m^3 and 100 mol/m^3 the Debye length ranges from approximately 1 nm to 10 nm (Jackson & Leinov, 2012), the minimum aperture in the REV should be $b_{min} > 0.4$ 10 m^{-6} for $l_D = 1$ nm and $b_{min} > 4$ 10 m^{-6} for $l_D = 10$ nm.

It is important to remark that Eq. (17) is almost identical to the equation obtained by Guarracino and Jougnot (2018) for the effective excess charge density $\hat{Q}_v^R$ carried by the water flow in a single capillary tube of radius R, which reads as follows:

$$\hat{Q}_v^R = \frac{8 N_A e_0 C^0}{(R/l_D)^2} \left[-2\frac{e_0\zeta}{k_B T} - \left(\frac{e_0\zeta}{3k_B T} \right)^3 \right]. \tag{18}$$

Note that the quotient between (17) and (18) yields to the following relation between the raduis R and the aperture b:

$$\frac{\hat{Q}_v^b}{\hat{Q}_v^R} = \frac{3}{2} \left(\frac{R}{b} \right)^2. \tag{19}$$

The above relation is identical to the one obtained by the quotient between the average velocity in the capillary tube (Poiseuille velocity) and the average velocity in the fracture given by (6), indicating that the effective excess charge strongly depends on the flow properties.

2.3 Electrokinetic properties of a fractured rock

In order to obtain the effective excess charge density in terms of the macroscopic hydraulic properties of the fractured rock, we consider the REV described in Section 1. Suppose that the fractured media is initially fully saturated and is drained by a tension head h (m). If we assume that the fractures drain at capillary pressure then the fracture of maximum aperture b_h drained by tension head h can be estimated as:

$$b_h = \frac{2\sigma \cos(\beta)}{\rho g_w h}. \tag{20}$$

Note that only the fractures of the REV which are fully saturated ($b_{min} \leq b \leq b_h$) contribute to water flow. Then the effective excess charge density of the fractured rock $\hat{Q}_v^{REV}$ can be computed as:

$$\hat{Q}_v^{REV} = \frac{1}{v_{BD} a^2} \int_{b_{min}}^{b_h} \hat{Q}_v^b \, \overline{v}(b) \, dA(b) \tag{21}$$

where $v_{BD} = \frac{\rho_w g}{\eta} k k_r(S) \frac{\Delta h}{a}$ is the Buckingham-Darcy's velocity (Buckingham, 1907), a^2 the cross-sectional area of the REV, and $dA(b)$ the area covered by fractures of aperture b defined by Eq. (4).

Substituting (17), (6) and (4) in (21) yields:

$$\hat{Q}_v^{REV} = N_A e_0 C^0 l_D^2 \left[-2\frac{e_0\zeta}{k_B T} - \left(\frac{e_0\zeta}{3k_B T} \right)^3 \right] \frac{a^{D-2}}{k k_r(S)} \left(b_h^{2-D} - b_{min}^{2-D} \right). \tag{22}$$

Table 1. Geometric and hydraulic parameters of fracture networks

	b_{max} (m)	b_{min} (m)	D (-)	ϕ (-)	k (m^2)	$\hat{Q}_v^{REV,sat}$ (C/m^3)
Fracture network 1	$8.0\,10^{-3}$	$8.0\,10^{-6}$	1.861	0.493	$2.76\,10^{-7}$	$1.010\,10^{-4}$
Fracture network 2	$5.7\,10^{-3}$	$5.7\,10^{-6}$	1.921	0.361	$8.88\,10^{-8}$	$2.304\,10^{-4}$
Fracture network 3	$4.4\,10^{-3}$	$4.4\,10^{-6}$	1.946	0.275	$3.82\,10^{-8}$	$4.082\,10^{-4}$

Finally, combining (7), (9) and (22) we obtain the following expression for $\hat{Q}_v^{REV}$:

$$\hat{Q}_v^{REV} = N_A e_0 C^0 l_D^2 \left[-2\frac{e_0\zeta}{k_B T} - \left(\frac{e_0\zeta}{3k_B T} \right)^3 \right] \frac{\phi S}{k k_r(S)}. \tag{23}$$

The equation (23) is the main finding of this study since it predicts the effective excess charge density from both electrokinetic and macroscopic hydraulic parameters such as ionic concentration, ζ-potential, Debye length, porosity, saturation and permeability. This equation is identical in form to the equation obtained by Soldi et al. (2018) for a porous medium described by a capillary tubes model with a fractal pore size distribution. Note that although the effective excess charge densities of both models at the pore scale and REV shapes are different, the expressions of effective excess charge density $\hat{Q}_v^{REV}$ in terms of macroscopic properties (ϕ, S, k and k_r) are identical. This result shows that Eq. (23) is valid for both sedimentary and fractured porous media. The overall dependence of the effective excess charge is also consistent with numerous previous studies (see a data compilation in Fig. 4.2 of Jougnot et al., 2020) and the empirical relationship proposed by Jardani et al. (2007).

To facilitate the analysis of the model we express $\hat{Q}_v^{REV}$ as the product of the saturated effective excess charge density $\hat{Q}_v^{REV,sat}$ (C/m^3) and the relative effective excess charge density $\hat{Q}_v^{REV,rel}$ (dimensionless):

$$\hat{Q}_v^{REV}(S) = \hat{Q}_v^{REV,sat} \hat{Q}_v^{REV,rel}(S) \tag{24}$$

where

$$\hat{Q}_v^{REV,sat} = N_A e_0 C^0 l_D^2 \left[-2\frac{e_0\zeta}{k_B T} - \left(\frac{e_0\zeta}{3k_B T} \right)^3 \right] \frac{\phi}{k}, \tag{25}$$

$$\hat{Q}_v^{REV,rel}(S) = \frac{S}{k_r(S)}. \tag{26}$$

Note that the relative effective excess charge density defined by Eq. 26 does not depend on electrokinetic parameters but only on hydraulic variables.

3 A synthetic example of fractured rocks

In this section, we predict the effective excess charge density for different fracture networks generated by Sierpinski carpets. Consider a cubic REV of side $a = 4$ cm and the patterns of fractures shown in Fig. 4, where the maximum apertures are successively reduced: a) $b_{max=}a/5$, b) $b_{max} = a/7$ and c) $b_{max} = a/9$. Fractal dimensions of Sierpinski carpet are estimated from (3). The minimum aperture b_{min} of each fracture network is considered to be 3 orders of magnitude less than the maximum aperture (i.e. $b_{min} = 10^{-3} b_{max}$). Porosity ($\phi$) and permeability ($k$) values are computed using (7) and (8). The geometric and hydraulic parameters of fracture networks are listed in Table 1. It can be observed that by reducing the aperture, the fractal dimension increases while both porosity and permeability decrease.

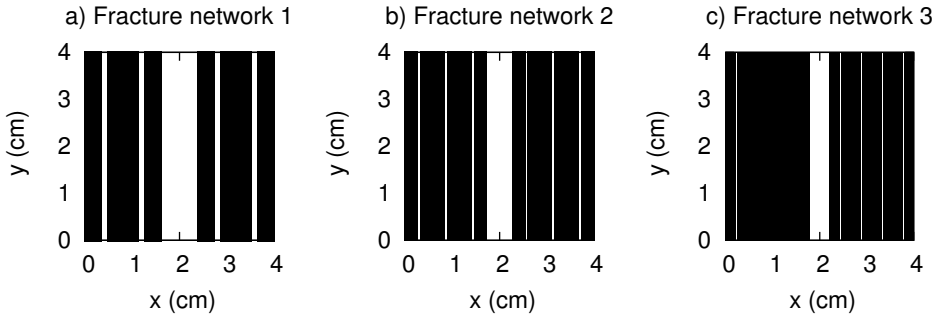

Figure 4. Parallel fracture networks generated by 2 recursion levels of Sierpinski carpets: (a) $D = 1.861$; (b) $D = 1.921$; (c) $D = 1.946$.

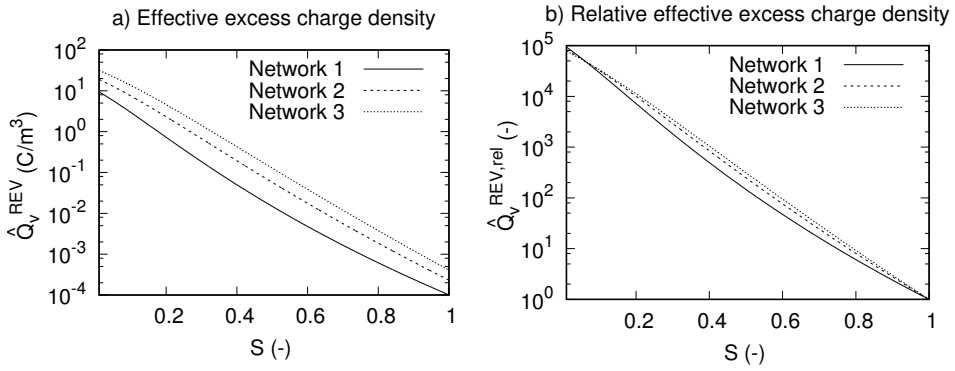

Figure 5. (a) Effective excess charge density versus saturation; (b) Relative effective excess charge density versus saturation.

To estimate the effective excess charge density we consider a ionic concentration $C^0 = 1$ mol/m^3, ζ-potential $\zeta = -0.07$ V and absolute temperature $T = 293.15$ K. The Debye length computed using (14) is $l_D = 9.65\,10^{-9}$ m, which is 3 orders of magnitude less than the minimum fracture aperture b_{min}. Saturated effective excess charge density values ($\hat{Q}_v^{REV,sat}$) are estimated from (25) and listed in Table 1. The values of $\hat{Q}_v^{REV,sat}$ increase the smaller the fracture apertures and the greater the number of fractures (see patterns of Fig. 4). Also note that fractal dimension D goes to 2 for small values of b_{max}.

Fig. 5 shows the influence of saturation degree on effective excess charge density $\hat{Q}_v^{REV}$ and relative density $\hat{Q}_v^{REV,rel}$ for the fracture networks depicted in Fig. 4. The values of $\hat{Q}_v^{REV}$ and $\hat{Q}_v^{REV,rel}$ increase approximately 5 orders of magnitude with the decrease of saturation. The maximum $\hat{Q}_v^{REV}$ value is reached when saturation tends to zero, i.e.:

$$\lim_{S\to 0} \hat{Q}_v^{REV}(S) = N_A e_0 C^0 l_D^2 \left[-2\frac{e_0\zeta}{k_B T} - \left(\frac{e_0\zeta}{3k_B T}\right)^3 \right] \frac{12}{b_{min}^2}. \tag{27}$$

Note that the maximum value of $\hat{Q}_v^{REV}$ depends on the electrokinetic parameters and on the factor $12/b_{min}^2$, which is the inverse of the permeability of the fractures with minimum aperture.

4 Application of the model to experimental self-potential data

In this section the saturated effective excess charge density model $\hat{Q}_v^{REV,sat}$ is confronted to the coupling coefficient C_c data obtained by Moore and Glaser (2007) for microcracked Sierra granite samples. These authors investigated the self potential response during hydraulic fracturing in the laboratory and determined C_c for different injection pressures. They found that C_c is approximately constant for pressures smaller than 2 MPa but then increases with pressure drop up to 80% just prior to hydraulic fracturing. This increasing C_c is related to the dilatancy of microcracks at high pressures, which causes an increase in permeability. In their study, permeability values are measured as a function of pressure drop (P) and the following exponential law is fitted to data:

$$k(P) = 10^{-18}\, e^{2.5\,10^{-4}\,P} \tag{28}$$

where k is in m^2 and P in kPa. The change of C_c with pressure drop P is described by the following best fit equation to seven samples of Sierra granite:

$$\Delta C_c(P) = 1.83\, e^{3.73\,10^{-4}\,P} \tag{29}$$

where ΔC_c is expressed as the percentage of the value of C_c at zero pressure drop. Prior to hydraulic fracturing the rock resistivity decreases by up to 2%, which is near to the practical limits of detection.

In order to apply our model to the data of Moore and Glaser (2007), C_c is estimated from $\hat{Q}_v^{REV,sat}$ by substituting (25) in (2):

$$C_c = N_A e_0 C^0 l_D^2 \left[-2\frac{e_0\zeta}{k_B T} - \left(\frac{e_0\zeta}{3k_B T}\right)^3 \right] \frac{\phi}{\sigma\eta}. \tag{30}$$

The coupling coefficient defined by Eq. (30) does not depend explicity on permeability, but on porosity. Unfortunately, the variation of porosity with pressure drop was not measured during the laboratory test. However, porosity can be estimated from permeability by combining Eq. (7) and (8). If we assume that $b_{min} << b_{max}$, the following relation is obtained:

$$\phi = \left[\frac{12(4-D)}{a^2(2-D)} k \right]^{\frac{2-D}{4-D}}. \tag{31}$$

Finally, combining (31), (28) and (30), and assuming that both the electrical conductivity and dynamic permeability do not depend on pressure, the following expression for the variation of C_c is obtained:

$$\Delta C_c(P) = 100 \left[\left(e^{2.5\,10^{-4}\,P} \right)^{\frac{2-D}{4-D}} - 1 \right]. \tag{32}$$

Note that the above equation is expressed as a percentage of the initial value and only depends on the fractal dimension D.

Figure 6 shows the fit of Eq. (32) to the experimental data obtained by Moore and Glaser (2007). If we assume a constant fractal dimension, the best fit of our model is obtained for D = 1.67 (solid line in Fig. 6). However, the fractal dimension is expected to vary with pressure P. The increase in permeability with P prior to hydraulic fracturing can be explained by dilatancy of microcracks (Moore & Glaser, 2007). According to our model, fractal dimension decreases with increasing aperture (see Table 1) and therefore with increasing pressure. Let us assume the following linear relationship between fractal dimension and pressure: $D(P) = 2 - \alpha P$, where α is a fitting parameter. This relationship for D provides a better fit of Eq. (32) to the experimental data, as is shown in Fig. 6 with a dashed line ($\alpha = 4.8\,10^{-5}$).

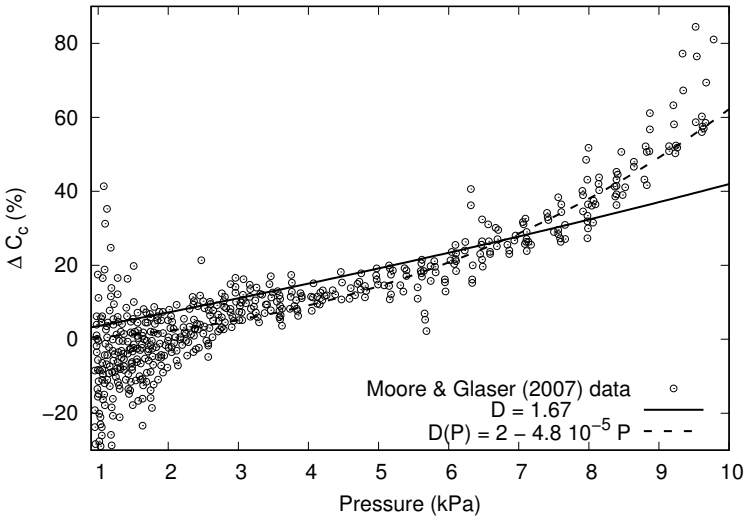

Figure 6. Variation of coupling coefficient with pressure $\Delta C_c(P)$. The empty circles are the experimental data obtained by Moore and Glaser (2007). The best fit of the proposed models to experimental data are displayed with solid (constant D) and dashed (D linearly dependent on P) lines.

5 Discussion and conclusions

In this study, we developped a fractal model to estimate the effective excess charge density in fully and partially saturated fractured rocks. The porous medium is described using the Sierpinski carpet, a classical fractal object that contains a self-similar geometric pattern of fractures. The mathematical procedures to estimate the effective parameters are based on the ideas presented in Guarracino and Jougnot (2018) for a classical capillary tubes model. The accuracy of the posed model has been tested to be correct for fracture apertures greater than 3 times the thickness of the electrical diffuse layer, i.e. $b > 3l_D$. This condition is fully satisfied under the thin double layer assumption which is valid for apertures $b > 400l_D$ (Jackson & Leinov, 2012).

The effective excess charge density model has a closed-form analytical expressions that depends on chemical parameters of the fracture water (ionic concentration, ζ-potential and Debye length) and hydraulic parameters (porosity, saturation and permeability). When expressed as these parameters, the model becomes identical to the ones derived by Guarracino and Jougnot (2018) and Soldi et al. (2018) for sedimentary porous media using capillary tubes. This result allows the extension of the validity of the models for classic porous media to fractured media. In addition, the model highlights the dependence of the effective excess charge density to the hydraulic properties. In this sense, Eq. (23) combined with the water flow models derived by Guarracino (2006) and Monachesi and Guarracino (2011) constitute a very good alternative to estimate the effective excess charge density since all the model expressions are obtained for the same fractal pattern of fractures. However, the proposed model can be combined with any constitutive model for water flow in fractured rocks (e.g., Guarracino & Quintana, 2009).

It is worth mentioning that due to the configuration of the geometry that we considered to develop the model, there is no exchange of water or ions between the fracture network and the matrix. This makes our model different from the numerical schemes proposed in Roubinet et al. (2016) or DesRoches et al. (2017). We redirect the reader to these references for fractured media in which this exchange occurs and cannot be neglected.

The synthetic tests show that the effective excess charge density increases with the decrease of both the fracture apertures and the degree of saturation. Finally, we show that the model is able to describe experimental data under fully saturated conditions for a published data set of coupling coefficient values measured in laboratory during hydraulic fracturing. Unfortunately, no experimental data are available to test model predictions under partially saturated conditions.

To the best of our knowledge, this is the first analytical model that consistently describes both electrokinetic and hydraulic properties in fully and partially saturated fractured rocks. The model provides simple explicit relations between effective excess charge density, porosity, permeability and saturation. These relations not only increase our general understanding of the electrokinetic phenomenon in fractured rocks, but also provide theoretical basis for quantitatively study of water flow using self-potential data.

Acknowledgments

The authors strongly thank the Editor, Lee Slater, and an anonymous reviewer for their very constructive comments on the original version of the manuscript. This research is partially supported by Universidad Nacional de La Plata, Consejo Nacional de Investigaciones Científicas y Técnicas (Argentina) and ANR EXCITING (grant ANR-17-CE06-0012).

Data Availability Statement

This theoretical paper only uses previously published data (Moore & Glaser, 2007). The Fortran source code to estimate the effective excess charge density in fractured rocks and coupling coefficient data extracted from Moore and Glaser (2007) have been archived in the Hydrogeophysics community of Zenodo and can be found at: `https://doi.org/10.5281/zenodo.5732504`.

References

Bodvarsson, G., Boyle, W., Patterson, R., & Williams, D. (1999). Overview of scientific investigations at yucca mountain—the potential repository for high-level nuclear waste. *Journal of Contaminant Hydrology*, *38*(1), 3-24. doi: https://doi.org/10.1016/S0169-7722(99)00009-1

Bonnet, E., Bour, O., Odling, N. E., Davy, P., Main, I., Cowie, P., & Berkowitz, B. (2001). Scaling of fracture systems in geological media. *Reviews of Geophysics*, *39*(3), 347-383. doi: https://doi.org/10.1029/1999RG000074

Buckingham, E. (1907). Studies on the movement of soil moisture. *Bureau of Soil Bulletin*, *38*, 29-61.

Corwin, R. F., & Morrison, H. F. (1977). Self-potential variations preceding earthquakes in central california. *Geophysical Research Letters*, *4*(4), 171-174. doi: https://doi.org/10.1029/GL004i004p00171

Demirel, S., Irving, J., & Roubinet, D. (2018). Comparison of rev size and tensor characteristics for the electrical and hydraulic conductivities in fractured rock. *Geophysical Journal International*, *216*(3), 1953-1973. doi: 10.1093/gji/ggy537

DesRoches, A. J., Butler, K. E., & MacQuarrie, K. T. (2017). Surface self-potential patterns related to transmissive fracture trends during a water injection test. *Geophysical Journal International*, *212*(3), 2047-2060. doi: 10.1093/gji/ggx528

Fagerlund, F., & Heinson, G. (2003). Detecting subsurface groundwater flow in fractured rock using self-potential (sp) methods. *Environmental Geology*, *43*, 782–794. doi: https://doi.org/10.1007/s00254-002-0693-x

Guarracino, L. (2006). A fractal constitutive model for unsaturated flow in fractured

hard rocks. *Journal of Hydrology*, *324*(1), 154-162. doi: https://doi.org/10.1016/j.jhydrol.2005.10.004

Guarracino, L., & Jougnot, D. (2018). A physically based analytical model to describe effective excess charge for streaming potential generation in water saturated porous media. *Journal of Geophysical Research: Solid Earth*, *123*(1), 52-65. doi: https://doi.org/10.1002/2017JB014873

Guarracino, L., & Quintana, F. (2009). A constitutive model for water flow in unsaturated fractured rocks. *Hydrological Processes*, *23*(5), 697-701. doi: https://doi.org/10.1002/hyp.7169

Helmholtz, H. (1879). Studien über electrische grenzschichten. *Annalen der Physik*, *243*(7), 337-382. doi: https://doi.org/10.1002/andp.18792430702

Hunter, R. J. (1981). *Zeta potential in colloid science*. Academic Press. doi: https://doi.org/10.1016/B978-0-12-361961-7.50004-3

Jackson, M. D., & Leinov, E. (2012). On the validity of the "thin" and "thick" double-layer assumptions when calculating streaming currents in porous media. *International Journal of Geophysics*, *2012*, 1-12. doi: https://doi.org/10.1155/2012/897807

Jardani, A., Revil, A., Bolv́e, A., Crespy, A., Dupont, J.-P., Barrash, W., & Malama, B. (2007). Tomography of the darcy velocity from self-potential measurements. *Geophysical Research Letters*, *34*(24). doi: https://doi.org/10.1029/2007GL031907

Jougnot, D., Linde, N., Revil, A., & Doussan, C. (2012). Derivation of soil-specific streaming potential electrical parameters from hydrodynamic characteristics of partially saturated soils. *Vadose Zone Journal*, *11*(1).

Jougnot, D., Mendieta, A., Leroy, P., & Maineult, A. (2019). Exploring the effect of the pore size distribution on the streaming potential generation in saturated porous media, insight from pore network simulations. *Journal of Geophysical Research: Solid Earth*, *124*(6), 5315-5335. doi: https://doi.org/10.1029/2018JB017240

Jougnot, D., Roubinet, D., Guarracino, L., & Maineult, A. (2020). Modeling streaming potential in porous and fractured media, description and benefits of the effective excess charge density approach. In B. A. & S. S. (Eds.), *Advances in modeling and interpretation in near surface geopyhsics*. Springer, Cham. doi: https://doi.org/10.1007/978-3-030-28909-6_4

Jougnot, D., Rubino, J. G., Carbajal, M. R., Linde, N., & Holliger, K. (2013). Seismoelectric effects due to mesoscopic heterogeneities. *Geophysical Research Letters*, *40*(10), 2033-2037. doi: https://doi.org/10.1002/grl.50472

Kormiltsev, V. V., Ratushnyak, A. N., & Shapiro, V. A. (1998). Three-dimensional modeling of electric and magnetic fields induced by the fluid flow movement in porous media. *Physics of the Earth and Planetary Interiors*, *105*(3), 109-118. doi: https://doi.org/10.1016/S0031-9201(97)00116-7

Leroy, P., & Revil, A. (2004). A triple-layer model of the surface electrochemical properties of clay minerals. *Journal of Colloid and Interface Science*, *270*(2), 371-380. doi: https://doi.org/10.1016/j.jcis.2003.08.007

Maineult, A., Thomas, B., Nussbaum, C., Wieczorek, K., Gibert, D., Lavielle, B., ... Lesparre, N. (2013). Anomalies of noble gases and self-potential associated with fractures and fluid dynamics in a horizontal borehole, mont terri underground rock laboratory. *Engineering Geology*, *156*, 46-57. doi: https://doi.org/10.1016/j.enggeo.2013.01.010

Medici, G., West, L., & Banwart, S. (2019). Groundwater flow velocities in a fractured carbonate aquifer-type: Implications for contaminant transport. *Journal of Contaminant Hydrology*, *222*, 1-16. doi: https://doi.org/10.1016/j.jconhyd.2019.02.001

Mizutani, H., Ishido, T., Yokokura, T., & Ohnishi, S. (1976). Electrokinetic phenomena associated with earthquakes. *Geophysical Research Letters*, *3*(7), 365-368.

doi: https://doi.org/10.1029/GL003i007p00365

Monachesi, L., & Guarracino, L. (2011). A fractal model for predicting water and air permeabilities of unsaturated fractured rocks. *Transport in Porous Media*, *90*, 779-789. doi: https://doi.org/10.1007/s11242-011-9815-9

Moore, J. R., & Glaser, S. D. (2007). Self-potential observations during hydraulic fracturing. *Journal of Geophysical Research: Solid Earth*, *112*(B2). doi: https://doi.org/10.1029/2006JB004373

Okubo, P. G., & Aki, K. (1987). Fractal geometry in the san andreas fault system. *Journal of Geophysical Research: Solid Earth*, *92*(B1), 345-355. Retrieved from `https://agupubs.onlinelibrary.wiley.com/doi/abs/10.1029/JB092iB01p00345` doi: https://doi.org/10.1029/JB092iB01p00345

Osiptsov, A. A. (2017). Fluid mechanics of hydraulic fracturing: a review. *Journal of Petroleum Science and Engineering*, *156*, 513-535. doi: https://doi.org/10.1016/j.petrol.2017.05.019

Rembert, F., Jougnot, D., & Guarracino, L. (2020). A fractal model for the electrical conductivity of water-saturated porous media during mineral precipitation-dissolution processes. *Advances in Water Resources*, *145*, 103742.

Ren, F., Ma, G., Wang, Y., Fan, L., & Zhu, H. (2017). Two-phase flow pipe network method for simulation of co2 sequestration in fractured saline aquifers. *International Journal of Rock Mechanics and Mining Sciences*, *98*, 39-53. doi: https://doi.org/10.1016/j.ijrmms.2017.07.010

Revil, A., & Jardani, A. (2013). *The self-potential method: Theory and applications in environmental geosciences*. Cambridge University Press.

Revil, A., & Leroy, P. (2004). Constitutive equations for ionic transport in porous shales. *Journal of Geophysical Research: Solid Earth*, *109*(B3). doi: https://doi.org/10.1029/2003JB002755

Revil, A., Linde, N., Cerepi, A., Jougnot, D., Matthäi, S., & Finsterle, S. (2007). Electrokinetic coupling in unsaturated porous media. *Journal of Colloid and Interface Science*, *313*(1), 315-327. doi: https://doi.org/10.1016/j.jcis.2007.03.037

Revil, A., Mao, D., Haas, A., Karaoulis, M., & Frash, L. (2015). Passive electrical monitoring and localization of fluid leakages from wells. *Journal of Hydrology*, *521*, 286-301. doi: https://doi.org/10.1016/j.jhydrol.2014.12.003

Rosas-Carbajal, M., Jougnot, D., Rubino, J. G., Monachesi, L., Linde, N., & Holliger, K. (2020). Seismoelectric signals produced by mesoscopic heterogeneities. In *Seismoelectric exploration* (p. 269-287). American Geophysical Union (AGU). doi: https://doi.org/10.1002/9781119127383.ch19

Roubinet, D., & Irving, J. (2014). Discrete-dual-porosity model for electric current flow in fractured rock. *Journal of Geophysical Research: Solid Earth*, *119*(2), 767-786. doi: https://doi.org/10.1002/2013JB010668

Roubinet, D., Linde, N., Jougnot, D., & Irving, J. (2016). Streaming potential modeling in fractured rock: Insights into the identification of hydraulically active fractures. *Geophysical Research Letters*, *43*(10), 4937-4944. doi: https://doi.org/10.1002/2016GL068669

Rubino, J. G., Guarracino, L., Muller, T. M., & Holliger, K. (2013). Do seismic waves sense fracture connectivity? *Geophysical Research Letters*, *40*(4), 692-696. doi: https://doi.org/10.1002/grl.50127

Shakas, A., Linde, N., Le Borgne, T., & Bour, O. (2018). Probabilistic inference of fracture-scale flow paths and aperture distribution from hydrogeophysically-monitored tracer tests. *Journal of Hydrology*, *567*, 305–319.

Sill, W. R. (1983). Self-potential modeling from primary flows. *GEOPHYSICS*, *48*(1), 76-86. doi: 10.1190/1.1441409

Smoluchowski, M. (1903). Contribution à la theórie de l'endosmose électrique et de quelques phenomènes corrélatifs. *Bulletin international de l'Académie des Sciences de Cracovie*, *8*, 182 – 200.

Sobolev, G. (1975). Application of electric method to the tentative short-term forecast of kamchatka earthquakes. *Pure and Applied Geophysics*, *113*, 229–235. doi: https://doi.org/10.1007/BF01592913

Soldi, M., Guarracino, L., & Jougnot, D. (2020). An effective excess charge model to describe hysteresis effects on streaming potential. *Journal of Hydrology*, *588*, 124949. doi: https://doi.org/10.1016/j.jhydrol.2020.124949

Soldi, M., Jougnot, D., & Guarracino, L. (2018). An analytical effective excess charge density model to predict the streaming potential generated by unsaturated flow. *Geophysical Journal International*, *216*(1), 380-394. doi: 10.1093/gji/ggy391

Tyler, S. W., & Wheatcraft, S. W. (1990). Fractal processes in soil water retention. *Water Resources Research*, *26*(5), 1047-1054. doi: https://doi.org/10.1029/WR026i005p01047

Wang, S., Wu, T., Cao, X., Zheng, Q., & Min, A. (2017). A fractal model for gas apparent permeability in microfractures of tight/shale reservoirs. *Fractals*, *25*(03), 1750036. doi: 10.1142/S0218348X17500360

Wishart, D. N., Slater, L. D., & Gates, A. E. (2006). Self potential improves characterization of hydraulically-active fractures from azimuthal geoelectrical measurements. *Geophysical Research Letters*, *33*(17). doi: https://doi.org/10.1029/2006GL027092

Wishart, D. N., Slater, L. D., & Gates, A. E. (2008). Fracture anisotropy characterization in crystalline bedrock using field-scale azimuthal self potential gradient. *Journal of Hydrology*, *358*(1), 35-45. doi: https://doi.org/10.1016/j.jhydrol.2008.05.017

Wu, H., Zhou, Y., Yao, Y., & Wu, K. (2019). Imaged based fractal characterization of micro-fracture structure in coal. *Fuel*, *239*, 53-62. doi: https://doi.org/10.1016/j.fuel.2018.10.117

Yoshida, S., Clint, O. C., & Sammonds, P. R. (1998). Electric potential changes prior to shear fracture in dry and saturated rocks. *Geophysical Research Letters*, *25*(10), 1577-1580. doi: https://doi.org/10.1029/98GL01222

Zhou, H., Zhong, J., Ren, W., Wang, X., & Yi, H. (2018). Characterization of pore-fracture networks and their evolution at various measurement scales in coal samples using x-ray ct and a fractal method. *International Journal of Coal Geology*, *189*, 35-49. doi: https://doi.org/10.1016/j.coal.2018.02.007